

Modeling interacting dynamic networks: III. Extraordinary properties in a population of extreme introverts and extroverts

Wenjia Liu¹, Florian Greil^{2,3}, K. E. Bassler^{2,3,4}, B. Schmittmann¹, and R. K. P. Zia^{1,4,5}

¹*Department of Physics and Astronomy, Iowa State University, Ames, IA 50011, USA*

²*Department of Physics, Department of Physics,
University of Houston, Houston, TX 77204, USA*

³*Texas Center for Superconductivity, University of Houston, Houston, TX 77204, USA*

⁴*Max-Planck-Institut für Physik komplexer Systeme,
Nöthnitzer Stra. 38, D-01187 Dresden, Germany and*

⁵*Department of Physics, Virginia Polytechnic Institute and State University, Blacksburg, VA 24061, USA*

E-mail: wjliu@iastate.edu, fgreil@uh.edu, bassler@uh.edu, schmittb@iastate.edu, rkpzia@vt.edu

Recently, we introduced dynamic networks with preferred degrees, showing that interesting properties are present in a single, homogeneous system as well as one with two interacting networks [22, 23]. While simulations are readily performed, analytic studies are challenging, due mainly to the lack of detailed balance in the dynamics. Here, we consider the two-community case in a special limit: a system of extreme introverts and extroverts - the *XIE* model. Surprising phenomena appear, even in this minimal model, where the only control parameters are the numbers of each subgroup: $N_{I,E}$. Specifically, an extraordinary transition emerges when N_I crosses N_E . For example, the fraction of total number of *I-E* links jumps from ~ 0 to ~ 1 . In a $N_I = N_E$ system, this fraction performs a pure random walk so that its distribution displays a *flat plateau* across most of $[0, 1]$, with the edges vanishing as $(N_{I,E})^{-0.38}$ for large systems. Thus, we believe the *XIE* model exhibits an ‘extreme’ Thouless effect [24]. For this limiting model, we show that detailed balance is restored and explicitly find the microscopic steady-state distribution. We then use a mean-field approach to find analytic expressions for the degree distributions that are in reasonably good agreement with simulations, provided N_I is not too close to N_E .

I. INTRODUCTION

For many years, there has been much interest in characterizing and understanding complex networks in nature [1–5]. While much of the venerable network literature is devoted to static aspects (e.g., graph theory), interest in their dynamic aspects began to emerge recently [6, 7], especially in the context of adaptive co-evolutionary networks [8, 9]. Now, in the settings of both artificial structures and natural environments, networks of very different kinds are intimately entangled, e.g., the internet and transportation networks, ocean currents and marine food-webs, etc. Thus, understanding how diverse, interdependent networks interact is also important. While some work along such lines [10–15] exists, the overall picture is far from clear. Within this context, our goal is modest: What are the effects of coupling *dynamic* networks of a similar type, but with different characteristics?

To focus our effort, we limit ourselves to a special class of dynamic networks, in which a node can cut or add links to the others. Various dynamics of this sort are possible. (See, for example, [16, 17].) Here, though, nodes alter their links in an attempt to achieve a ‘preferred’ number (κ) of connections. We believe that the notion of preferred degrees is particularly suitable for modeling networks in a social setting, in which introverts/extroverts are naturally inclined to have few/many contacts. While such a model may be applicable to the dynamics of opinion formation, it is also ideal for studying the effects of self-imposed or public policies, in the event of an epidemic outbreak, by including a time dependent κ . Thus,

an individual’s preferred degree may drop by an order of magnitude or more, e.g., from hundreds of contacts during a typical day, to just a few family members or care-givers.

Introduced a few years ago [18–21], we recently began more systematic studies on interacting networks with preferred degrees, the present being the third of a series. In the first [22], we provided specifics of how to implement a preferred degree for a homogeneous population of individuals, introducing various natural ways to incorporate the action of cutting/adding a link. With simple arguments, we can predict the degree distribution, $\rho(k)$, which agrees well with simulation results. To model interactions, we considered two such communities, with different numbers ($N_{1,2}$) and κ ’s, and introduced a simple way to couple them: When a node attempts to add/cut a link, it chooses a partner from the other community with probability χ (and an intra-community partner with $1 - \chi$) for the action. Though such a model seems minimal, the complexities involved include a six-dimensional parameter space ($N_{1,2}, \kappa_{1,2}, \chi_{1,2}$) and the presence of four degree distributions of interest (associated with intra- and inter-community links). Despite its simplistic appearance, this model displays some surprising phenomena. In the second of the series [23], we performed a more detailed study in a wider region of parameter space and arrived at some general principles to predict the observed behavior. Nevertheless, since the dynamics does not obey detailed balance, determining the microscopic distribution in the stationary state (\mathcal{P}^{ss} , à la the Boltzmann distribution for systems in equilibrium) is a major challenge, let alone computing averages of macroscopic

observables. In this paper, we consider a special limit of a system with two communities. Dubbed the *XIE* model, it consists of a collection of *eXtreme Introverts* and *Extroverts*, whose only action is either cutting a link or making one. This simplifying assumption means the model has only two control parameters, $N_{I,E}$, the number of introverts and extroverts. As the $N_I = N_E$ line is crossed, a remarkably sharp transition emerges. It turns out that detailed balance is restored in this limit and so, we are able to arrive at an explicit expression for \mathcal{P}^{ss} . Though computing averages with \mathcal{P}^{ss} is still difficult, various mean-field techniques can be applied and some aspects of this model can be well understood. In particular, the transition appears to be of mixed order and is likely to be in the class of an ‘extreme’ Thouless effect [24]. While preliminary results have been reported earlier [20, 25], we will present a more systematic study of this model here.

The rest of this paper is organized as follows. In the next section, we provide a detailed description of the model, the master equation associated with the stochastic process, and the exact microscopic distribution in the steady state. The following section is devoted to studies of the degree distributions, through both Monte Carlo simulations and a self-consistent mean-field theory. In simulations with $N_I + N_E$ fixed at 200 and varying $N_I - N_E$, we find good agreement with the theory *except* the $N_I = N_E = 100$ case. This surprising result leads us to explore, in Section 4, the behavior of a genuinely macroscopic quantity, X , the total number of cross-links. We end with a summary and outlook.

II. A MODEL OF EXTREME INTROVERTS AND EXTROVERTS

In our previous studies [22, 23], we introduced adaptive networks in which each node adds/cuts links to other nodes according to its ‘preferred degree’ (κ) for both a homogeneous population and a heterogeneous system of two communities with different characteristics (e.g., numbers of nodes and κ ’s). For the reader’s convenience, we summarize briefly here the specifications and the findings for the simplest model, the extreme limit of which is the focus of this study.

First, we consider a homogeneous population consisting of a dynamic set of links among N nodes, all of which are assigned the same κ . In each time step, a random node is chosen and its degree, k , is noted. If $k > \kappa$, the node cuts one of its existing links at random. Otherwise, it adds a link to a randomly chosen node not connected to it. (Models with more ‘flexibility’ in the nodes were studied in [22].) This simple stochastic process is ergodic, so that the system eventually settles into a unique stationary distribution, $\mathcal{P}^{ss}(\mathbb{A})$ over the space of networks – symmetric $N \times N$ adjacency matrices, \mathbb{A} . Despite the apparent randomness, the resulting degree distribution is a Laplacian, $\rho(k) \propto \exp[-|k - \kappa| \ln 3]$, which differs considerably from the binomial distribution (i.e., Gaussian or Poisson, in the limit of large N) in Erdős-Rényi graphs

[26]. Second, since our goal is interaction of networks, we turn to a study of two networks of preferred degrees. Assuming that $\kappa_1 < \kappa_2$, naturally we refer to the first group as ‘introverts’ (I) and the later one as ‘extroverts’ (E). To model the interaction between these groups, we introduced a simple parameter $\chi \in [0, 1]$, which is the probability for the chosen node to take action (adding or cutting) on a cross-link. Letting $\chi_1 \neq \chi_2$ as well as $N_1 \neq N_2$, we find a variety of behaviors [23], some of which can be understood, at least qualitatively. The most surprising phenomenon observed concerns the statistical properties of the number of cross-links, X . Specifically, we simulated two communities with identical properties: $N_{1,2} = 100, \kappa_{1,2} = 25, \chi_{1,2} = 0.5$. In the stationary state, the distribution of X (dropping superscript *ss* for simplicity and denoted by $P(X)$) displays a very broad and flat plateau. By contrast, we can arbitrarily partition a *homogeneous* population of $N = 200$ into two equal halves. Using $\kappa = 25$ and defining X as the number of links between the halves, we find that $P(X)$ is just a binomial distribution, with easily predictable parameters. As the standard deviation of the former is an order of magnitude larger than the binomial, it is clear that, despite its conceptual simplicity, coupling two networks via χ has a profound effect on the system.

The underlying dynamics of these systems violates detailed balance. As a result, the stationary state will be a non-equilibrium steady state (NESS), in the sense that persistent probability currents will prevail [27]. Thus, we encounter serious challenges in our attempts to understand analytically these dramatically different behaviors. Nevertheless, we believe some insight into our interacting networks can be gained by turning to limiting cases which embody the main features of the full system. In this spirit, we consider the ultimate limit: $\kappa_1 = 0, \kappa_2 = \infty$. In other words, these are extreme introverts and extroverts (or *XIE*, for short). The rules cannot be simpler: When chosen to act, an introvert will cut a random existing link, while an extrovert will add a link to a random individual in the population not already connected. To implement Monte Carlo simulations, one significant simplification is evident. The two intra-communities will quickly end in a null and a complete graph, and only the *I-E* cross-links are dynamic. With all intra-community links frozen (as illustrated in Fig. 1), our active network reduces to bipartite graphs and the configuration space of our system reduces to incidence matrices, \mathbb{N} , i.e., a $N_I \times N_E$ rectangle in the full adjacency matrix, \mathbb{A} . Therefore, instead of having to consider $2^{N(N-1)/2}$ configurations, we can focus on only $2^{\mathcal{N}}$ configurations, where

$$\mathcal{N} \equiv N_I N_E \quad (1)$$

is the maximum number of cross-links allowed. Given the evolution rules, there are only two control parameters, N_I and N_E , in our model. Though this system may appear to be minimal and devoid of interest, we find surprising features associated with X as well as the degree distributions. In particular, there is an extraordinary phase boundary along the $N_I = N_E$ line.

Let us denote an element of \mathbb{N} by n_{ij} , which is 1 or 0 when the link between an introvert node i and an extrovert j is present or absent, respectively. Clearly, $i \in [1, N_I]$ and $j \in [1, N_E]$. From the microscopic n_{ij} , various quantities of interest can be formed, e.g., $X = \sum_{ij} n_{ij}$. At another level, the degree of an I (E) node, can be obtained by summing n along a row (column). To expose a not-so-explicit symmetry, we consider the *complement* of a degree, namely, the number of links (associated with a particular node) *less* than the maximum possible value (i.e., $N - 1 - k$). This measure is especially suited for characterizing an E node. Letting $\bar{n}_{ij} \equiv 1 - n_{ij}$, we define

$$k_i \equiv \sum_j n_{ij}; \quad p_j \equiv \sum_i \bar{n}_{ij} \quad (2)$$

which are the degree of an I node i and the complement of the degree of an E node j , respectively. Note that, for the XIE model, $k_i \in [0, N_E]$ and $p_j \in [0, N_I]$. Meanwhile, the dynamics correspond to changing an element of \mathbb{N} from 1 to 0 or vice versa. Mapping this binary variable to ± 1 , our model becomes a kinetic Ising model with spin flip dynamics [28]. In the lattice gas language [29], k_i is the number of particles in row i , while p_j is the number of holes in column j . Similar to the Ising case (but with an additional exchange operation), the key symmetry here is

$$n_{ij} \Leftrightarrow \bar{n}_{ji} \oplus N_I \Leftrightarrow N_E \quad (3)$$

which we will refer to as ‘particle-hole symmetry.’ A layman’s way to phrase this symmetry is: The presence of a link is as intolerable to an introvert as the absence of one (i.e., presence of a ‘hole’) to an extrovert. This symmetry will play an important role in discussions below. In particular, it behooves us to characterize the state of an extrovert by a ‘hole distribution’

$$\zeta(p) = \rho(N - 1 - p) \quad (4)$$

rather than the standard degree distribution, $\rho(k)$.

A. Master equation and the exact microscopic steady state distribution

A complete analytical description of the XIE model is given by $\mathcal{P}(\mathbb{N}, t | \mathbb{N}_0, 0)$, which is the probability of finding the system in configuration \mathbb{N} after t steps, starting with initial configuration \mathbb{N}_0 . (In simulations, we typically let \mathbb{N}_0 be the null matrix or a randomly half filled one. But, since our main interest will be properties of the stationary state, we will drop the $\mathbb{N}_0, 0$ part.) The discrete master equation for \mathcal{P} can be written:

$$\mathcal{P}(\mathbb{N}, t+1) - \mathcal{P}(\mathbb{N}, t) = \sum_{\{\mathbb{N}'\}} [W(\mathbb{N}, \mathbb{N}') \mathcal{P}(\mathbb{N}', t) - W(\mathbb{N}', \mathbb{N}) \mathcal{P}(\mathbb{N}, t)] \quad (5)$$

where $W(\mathbb{N}, \mathbb{N}')$ is the probability for configuration \mathbb{N}' to become \mathbb{N} in a step (attempt). Using (2), $W(\mathbb{N}', \mathbb{N})$ can

be easily written:

$$\sum_{i,j} \frac{\Delta}{N} \left[\frac{\Theta(k_i)}{k_i} \bar{n}'_{ij} n_{ij} + \frac{\Theta(p_j)}{p_j} n'_{ij} \bar{n}_{ij} \right] \quad (6)$$

where $\Theta(x)$ is the Heavyside function (i.e., 1 if $x > 0$ and 0 if $x \leq 0$) and $\Delta \equiv \prod_{k\ell \neq ij} \delta(n'_{k\ell}, n_{k\ell})$ ensures that only n_{ij} may change in a step. With such a random sequential scheme, each node has an even chance of being chosen after N attempts. Thus, N attempts is often referred to as one Monte Carlo step (MCS), so that a run of τ MCS involves τN ‘spin-flip attempts.’

The dynamics defined here is clearly ergodic. More remarkable is that it obeys detailed balance, as shown in Appendix A. Consequently, in the $t \rightarrow \infty$ limit, \mathcal{P} approaches a unique stationary distribution, \mathcal{P}^{ss} , while all probability currents vanish. More crucially, detailed balance allows us to find \mathcal{P}^{ss} by applying $\mathcal{P}^{ss}(\mathbb{N}) = \mathcal{P}^{ss}(\mathbb{N}') W(\mathbb{N}, \mathbb{N}') / W(\mathbb{N}', \mathbb{N})$ repeatedly. Imposing normalization, we arrive at an explicit closed form:

$$\mathcal{P}^{ss}(\mathbb{N}) = \frac{1}{\Omega} \prod_{i=1}^{N_I} (k_i!) \prod_{j=1}^{N_E} (p_j!) \quad (7)$$

where $\Omega = \sum_{\{\mathbb{N}\}} \prod (k_i!) \prod (p_j!)$ is a ‘partition function.’ Note that the particle-hole symmetry (c.f. Eqn. 3) is manifest here.

Interpreting \mathcal{P}^{ss} as a Boltzmann factor, we can write a ‘Hamiltonian’ [36]

$$\mathcal{H}(\mathbb{N}) = - \left\{ \sum_{i=1}^{N_I} \ln \left(\sum_{j=1}^{N_E} n_{ij} \right)! + \sum_{j=1}^{N_E} \ln \left(\sum_{i=1}^{N_I} \bar{n}_{ij} \right)! \right\} \quad (8)$$

Now, this form immediately alerts us to the level of complexity of this system of ‘Ising spins,’ as \mathcal{H} contains a peculiar form of long range interactions. Each ‘spin’ is coupled to all other ‘spins’ *in its row and column*, via all possible types of ‘multi-spin’ interactions! We are not aware of any system in solid state physics with this kind of interactions. Yet, \mathcal{H} exposes the underlying structure of (a limit of) a very simple model of social interactions. Meanwhile, it is understandable that computing Ω , let alone statistical properties of macroscopic quantities, will be quite challenging. Nevertheless, as the next two sections show, we are able to exploit mean-field approaches to predict various quantities, for generic points in the space of control parameters: (N_I, N_E) . As in standard equilibrium statistical systems, our mean-field theory fails in the neighborhood of critical points, which turn out to be the $N_I = N_E$ line here.

III. DEGREE DISTRIBUTIONS: SIMULATION RESULTS AND THEORETICAL CONSIDERATIONS

In this section, we focus on a quantity most commonly studied in networks: the degree distribution, $\rho(k)$. Of

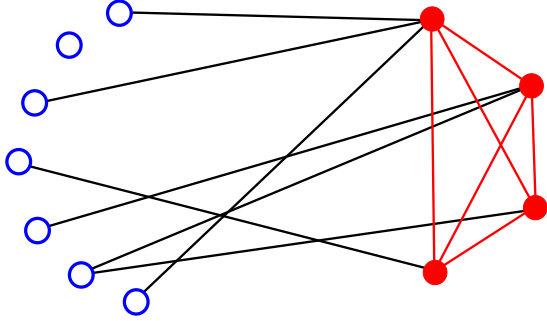


FIG. 1: The nodes of the two groups are denoted by circles: blue open (I) and red closed (E). The black lines represent the active cross-links and the red lines, the frozen E - E links. For this network, the sets of k 's are: $k_I = \{1, 0, 1, 1, 1, 2, 1\}$, and $k_E = \{6, 5, 4, 4\}$. Thus, this configuration contributes 1, 5, 1 to ρ_I ($k=0, 1, 2$) and 2, 1, 1 to ρ_E ($k=4, 5, 6$), respectively.

course, there are several types of ρ 's for a system with G subgroups or communities. If k_{AB} denotes the number of nodes in group B connected to a node in group A (i.e., the links A has to B), then, in general, $\langle k_{AB} \rangle \neq \langle k_{BA} \rangle$. Instead, we have $N_A \langle k_{AB} \rangle = N_B \langle k_{BA} \rangle$ as the average number of all the links between subgroups A and B , while the numbers of nodes in each, N_A and N_B , are not necessarily equal. Thus, we have G^2 degree distributions in general. For XIE however, the internal links, k_{AA} , are static with trivial distributions (e.g., $\delta(k_{II})$). Thus, it is sufficient to describe each subgroup by just one degree distribution, associated with k_{IE} and k_{EI} . For simplicity, we will denote these as $\rho_I(k_I)$ and $\rho_E(k_E)$, respectively (e.g., $\rho_I(1) = 5$ and $\rho_E(6) = 1$ in Fig. 1). In view of the particle-hole symmetry discussed above, we will often consider $\zeta_E(p_E)$ instead.

A. Simulation results for ρ_I and ρ_E

Our main goal is to demonstrate that interesting phenomena can emerge from a minimal model like XIE , and that they can be understood reasonably well by mean-field analysis, rather than a systematic and exhaustive study of this particular system. Thus, we restrict our simulation studies mainly to $N = N_I + N_E = 200$, a number large enough to show collective behavior, yet small enough for gathering good statistics. Starting with a network with various initial conditions (null graph, complete graph, random half-filled), we evolve the system according to the simple rules given above. Not surprisingly, after $O(N)$ MCS, all the I - I links are absent while all the E - E links are present. To be quite certain that the system has equilibrated, we discard the first 5×10^7 MCS. Thereafter, we measure the degrees of each node every 50 MCS. The distributions are then obtained as the average over 10^8 measurements. As our main focus is not the transient behavior, but rather only steady state proper-

ties, we will drop the superscripts ss to simplify notation.

The degree distributions, $\rho(k)$, for three cases – $(N_I, N_E) = (150, 50)$, $(125, 75)$, $(101, 99)$ – are shown in Fig. 2(a). Evidently, each ρ consists of two disjoint components, associated with small/large k . It is clear that, since the I 's are only linked to the E 's, the distribution associated with $k \leq N_E$ can be attributed to $\rho_I(k_I)$. Similarly, since all E - E links are present, $\rho_E(k_E)$ can be identified with the component with $k \geq N_E - 1$. For these cases, there is no overlap at $k = N_E - 1, N_E$ so that we can label ρ_I and ρ_E without ambiguity: open and solid symbols respectively. Apart from having these two components, the most prominent feature is that neither component resembles $3^{-|k-\kappa|}$, the degree distribution of a homogeneous population with preferred degree κ [19, 22]. As will be shown, they are well approximated by Poisson distributions, the analytic result of a mean-field approach.

Of course, the averages obey $\langle k_I \rangle < \langle k_E \rangle$, especially since they must satisfy

$$\langle k_I \rangle N_I = (\langle k_E \rangle - N_E + 1) N_E \quad (9)$$

which is the average of the total number of cross-links: $\langle X \rangle$. Meanwhile, we can expect that, since each node is given the same chance to act, all these averages will increase as the ratio N_E/N_I increases. Other than these obvious aspects, a casual glance shows several surprising features. For example, $\langle k_I \rangle \cong 0.5, 1.4$, and 13.9 for the ρ_I 's in Fig. 2(a), associated with, respectively, $N_E/N_I = 1/3, 3/5$, and $99/101$. Naively, N_E/N and N_I/N may be thought of as the probability of adding and cutting a cross-link, leading to the expectation that the ratio $\langle X \rangle / [N - \langle X \rangle]$ (presence/absence of link) is N_E/N_I . A little algebra leads further to the prediction $\langle k_I \rangle = N_E^2/N$, i.e., approximately 12.5, 28.1, and 49.0. Needless to say, this naive picture is far from realized.

Before considering a more successful theoretical approach, we present the system's behavior for $N_I < N_E$. In Fig. 2(b), we illustrate the degree distribution for $(N_I, N_E) = (99, 101)$ (blue circles), as well as the previous case of $(101, 99)$ (green circles). In other words, just two introverts have 'changed sides' here. The first remarkable feature is the sizeable jump, easily discerned by focusing on say, the two ρ_I 's, shown with open symbols. The other notable feature is the symmetry, which can be traced to the underlying 'particle-hole symmetry.' By exchanging $N_I \leftrightarrow N_E$ and plotting the degree distribution *vs.* $p \equiv N - 1 - k$, we find excellent overlap between the blue and green data points. Of course, such a plot displays $\zeta(p)$, the 'hole distribution.'

Finally, let us turn to the symmetric case $(100, 100)$, which appears to be most challenging, for both Monte Carlo simulations and theoretical understanding. First of all, the run time it takes for the system to settle is much longer, typically a hundred-fold longer than the $N_I \neq N_E$ cases. To compile a reliable histogram for the $\rho(k)$, shown in Fig. 3, we take 10^{10} measurements in a combination of 5 runs, each of which lasts for 10^{11} MCS (after discarding the first 10^7 MCS for the system to settle into steady states). Note that, to untangle $\rho_{I,E}$ in

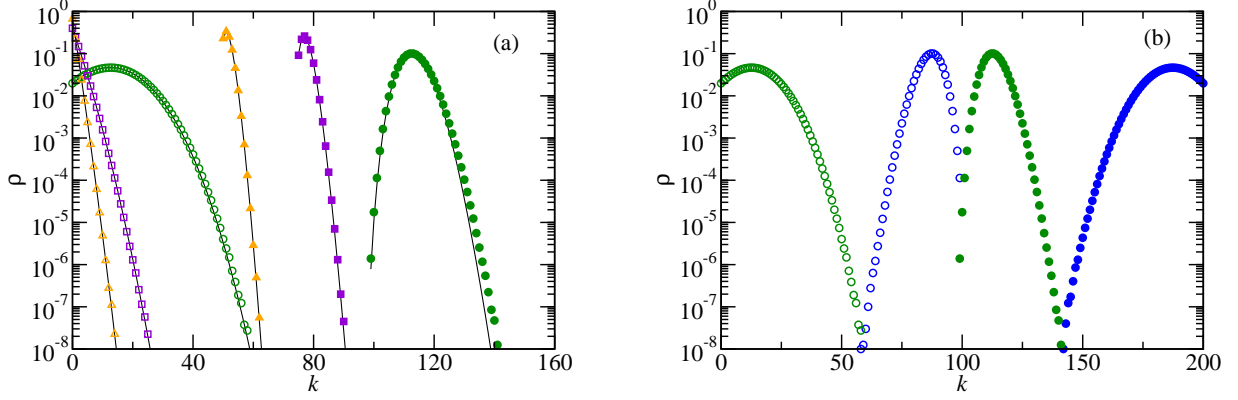


FIG. 2: Degree distributions, ρ , for several cases with $N_I + N_E = 200$. Simulation results for the low/high k components, associated with introverts/extroverts, are denoted by open/solid symbols. (a) The symbols for (N_I, N_E) are orange triangles (150, 50), purple squares (125, 75), and green circles (101, 99). The solid black lines are predictions from a self-consistent mean-field theory. (b) When two introverts ‘change sides,’ a dramatic jump in $\rho(k)$ results, with the case of (99, 101) shown as blue circles.

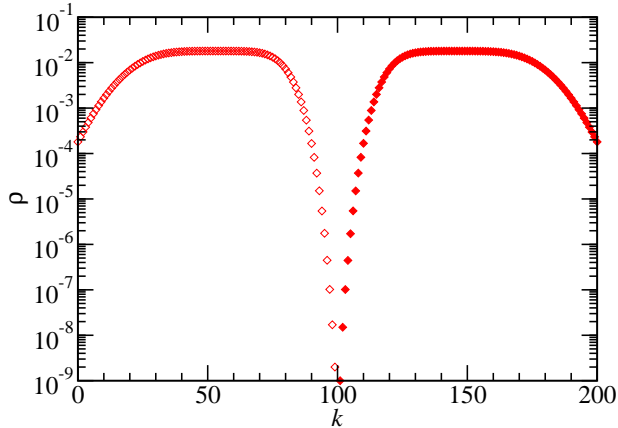


FIG. 3: Simulation results of the degree distribution for the symmetric (100, 100) case. The two components, denoted by open and solid diamonds, can be associated with the separate distributions ρ_I and ρ_E , respectively.

the central pair of points, we recorded separately whether an I or a E node has 99, 100 links. Of course, the distribution is symmetric, i.e., $\rho_I = \zeta_E$. The unexpected aspect is the presence of broad and flat plateaux, quantitative understanding of which remains elusive. As will be discussed in Section 4, models with $N_I = N_E$ can be regarded as critical systems in which large fluctuations and critical slowing down can be typically expected. In the next subsection, we will sidestep this problematic case and focus only on systems with $N_I \neq N_E$, for which a mean-field approach proves to be quite successful.

B. Self-consistent mean-field approximation

Given the exact steady state distribution (Eqn. (7)), the ρ 's can be computed, in principle, via

$$\rho_I(k_I) = \sum_{\{\mathbf{N}\}} \delta(k_I - \sum_j n_{ij}) \mathcal{P}^{ss}(\mathbf{N}) \quad (10)$$

$$\rho_E(k_E) = \sum_{\{\mathbf{N}\}} \delta(k_E - \sum_i n_{ij}) \mathcal{P}^{ss}(\mathbf{N}) \quad (11)$$

(for any i in the first equation and any j in the second). In practice, this task is extremely challenging. In particular, since $k_{I,E}$ correspond to, in a 2-dimensional Ising model, the total magnetization in a row or a column, it is understandable that computing their full *distributions* is beyond our reach. Thus, we resort to a mean-field approach, applied to the underlying *dynamics* of the model [22, 23]. In other words, we implement an approximation scheme on the transition probabilities for the degree of a *particular* node to increase/decrease by unity: $R(k \rightarrow k \pm 1)$. Once these are determined, the *approximate* (signified with a tilde above) steady state degree distribution must satisfy

$$\tilde{\rho}(k) R(k \rightarrow k-1) = \tilde{\rho}(k-1) R(k-1 \rightarrow k) \quad (12)$$

and can be found in closed form.

Specifically, we first consider a particular I node, with $\rho_I(k_I)$ being the probability to find it having k_I links. Then, provided $k_I > 0$, $R_I(k_I \rightarrow k_I - 1) = 1/N$ which is the probability that this node is chosen to act. By contrast, the exact rate for having a link added ($k_I - 1 \rightarrow k_I$) is more complicated, since it depends not only on all the $N_E - k_I + 1$ extroverts *not* connected to it, but also on how many ‘holes’ each has – through $1/p_j$ (in Eqn. (6)). To proceed, we must make judicious approximations. In the spirit of mean-field theory, we can replace $1/p_j$ by the average $\langle 1/p_E \rangle'$, where the prime stands for an average *restricted* to nodes with $p_E > 0$. Though we can

formulate the theory with $\langle 1/p_E \rangle'$, let us make a further simplifying approximation and replace it by $1/\langle p_E \rangle'$. So, we write

$$R_I(k_I - 1 \rightarrow k_I) \cong \frac{N_E - k_I + 1}{N} \frac{1}{\langle p_E \rangle'} \quad (13)$$

If we had the distribution of an extrovert's holes, $\zeta_E(p_E)$, then we have the following relation:

$$\langle p_E \rangle' \equiv \frac{\sum_{p_E > 0} p_E \zeta_E(p_E)}{\sum_{p_E > 0} \zeta_E(p_E)} = \frac{\langle p_E \rangle}{1 - \zeta_E(0)} \quad (14)$$

Of course, since $\rho_E(k_E)$ is unknown, so is $\zeta_E(p_E)$. As will be shown, the goal of a self-consistent mean-field theory is to find an approximate expression for these distributions, as well as for ρ_I .

Proceeding, we exploit Eqn. (12) and readily find

$$\begin{aligned} \tilde{\rho}_I(k_I) &= \frac{N_E - k_I + 1}{\langle p_E \rangle'} \frac{N_E - k_I + 2}{\langle p_E \rangle'} \dots \frac{N_E}{\langle p_E \rangle'} \tilde{\rho}_I(0) \\ &\propto \frac{(\langle p_E \rangle')^{N_E - k_I}}{(N_E - k_I)!} \end{aligned} \quad (15)$$

Since $p_I \equiv N_E - k_I$ is the number of 'holes' associated with an I node, we recognize this as a Poisson distribution (truncated at N_E) for the hole distribution. Imposing normalization, we find a compact closed form, $\tilde{\zeta}_I(p_I) = (\langle p_E \rangle')^{p_I} / Z_I p_I!$, where $Z_I = \sum_{\ell=0}^{N_E} (\langle p \rangle')^\ell / \ell!$ is the sum of the first $N_E + 1$ terms of an exponential series. Despite its simplicity, we feel that the notation $\tilde{\zeta}_I(p_I)$ may be too confusing and so, we will remain with $\tilde{\rho}_I$ instead:

$$\tilde{\rho}_I(k_I) = \frac{(\langle p_E \rangle')^{N_E - k_I}}{Z_I (N_E - k_I)!} \quad (16)$$

Of course, $\langle p_E \rangle'$ is still an unknown parameter at this point. For that, we turn to a particular E node and, exploiting 'particle-hole' symmetry, consider its hole distribution, $\zeta_E(p_E)$. Since adding a link is decreasing p_E by unity, we again have $R_E(p_E + 1 \rightarrow p_E) = 1/N$, the probability that this node is chosen to act, provided $p_E > 0$. Meanwhile, it is connected to $N_I - p_E$ (i.e., $k_E - N_E + 1$) introverts, each of which has k_i links. As above, we rely on the same arguments and replace the k_i 's by a suitable average:

$$R_E(p_E \rightarrow p_E + 1) \cong \frac{N_I - p_E}{N} \frac{1}{\langle k_I \rangle'} \quad (17)$$

where

$$\langle k_I \rangle' = \frac{\langle k_I \rangle}{1 - \rho_I(0)} \quad (18)$$

Recasting Eqn. (12) for $\tilde{\zeta}$, we have

$$\tilde{\zeta}_E(p_E) = \frac{\langle k_I \rangle'}{N_I - p_E} \tilde{\zeta}_E(p_E + 1) \quad (19)$$

This recursion relation leads to a (truncated) Poisson distribution in $N_I - p_E$, and imposing normalization, we have

$$\tilde{\zeta}_E(p_E) = \frac{(\langle k_I \rangle')^{N_I - p_E}}{Z_E (N_I - p_E)!} \quad (20)$$

with $Z_E = \sum_{\ell=0}^{N_I} (\langle k \rangle')^\ell / \ell!$. Of course, we recognize $N_I - p$ is just the number of *cross*-links associated with a E node: $k_E - N_E + 1$. Thus, the expression for $\tilde{\rho}_E(k_E)$ will not be simpler. Note that, along with Eqn. (16), this result again confirms the underlying particle-hole symmetry.

Though $\langle k_I \rangle'$ is also an unknown, we can compute both it and $\langle p_E \rangle'$ using the approximate distributions $\tilde{\rho}_I$ and $\tilde{\zeta}_E$ in Eqns. (18,14) instead. Since $\tilde{\rho}_I$ and $\tilde{\zeta}_E$ depend on $\langle p_E \rangle'$ and $\langle k_I \rangle'$, respectively, we may define the functions f and g :

$$\begin{aligned} \langle k_I \rangle' &\cong \frac{\sum k_I \tilde{\rho}_I(k_I)}{1 - \tilde{\rho}_I(0)} \equiv f(\langle p_E \rangle'); \\ \langle p_E \rangle' &\cong \frac{\sum p_E \tilde{\zeta}_E(p_E)}{1 - \tilde{\zeta}_E(0)} \equiv g(\langle k_I \rangle') \end{aligned} \quad (21)$$

Making a plot of these functions in the $\langle k \rangle'$ - $\langle p \rangle'$ plane, the point of intersection then determines, self-consistently, the values for these two parameters. In practice, it is simple to start with, say, a trial value p_0 for $\langle p_E \rangle'$ and compute $\langle k_I \rangle'$ through Eqn. (16). Inserting this $\langle k_I \rangle'$ into Eqn. (20), we compute $\tilde{\zeta}_E$ and the associated $\langle p_E \rangle'$. If this result is not p_0 , then vary the latter until they agree. In other words, this process will find the solution to $\langle p_E \rangle' = g(f(\langle p_E \rangle'))$. Instead of quoting the self consistent values for $\langle p_E \rangle'$ and $\langle k_I \rangle'$, we plot the full distributions predicted by Eqns. (20,16), shown as solid black lines in Fig. 2(a). We should emphasize that *no* fit parameters have been introduced in this approach; the lines depend only on the control parameters, $N_{I,E}$. It is clear that the agreement between theory and simulation data is excellent for $N_I/N_E \gg 1$. By symmetry, it will also be quite good for cases with $N_I \ll N_E$. For the (101,99) case, disagreement between theory and data is visibly detectable, a sign that correlations are no longer negligible. We did not plot the predictions for the $N_I = N_E = 100$ case, as the theory is, not surprisingly, deficient.

While there is reasonably good agreement between this theory and simulation data for systems with $N_I \neq N_E$, it does not offer much insight into the dramatic changes when just two individuals 'change sides,' nor the emergence of broad plateau in Fig. 3. To address some of these issues, we turn next to a more macroscopic perspective, focusing only on the total number of cross-links, X .

IV. STATISTICAL PROPERTIES OF X , THE TOTAL NUMBER OF CROSS-LINKS

Though degree distributions are standard for characterizing networks, the puzzling features displayed in the

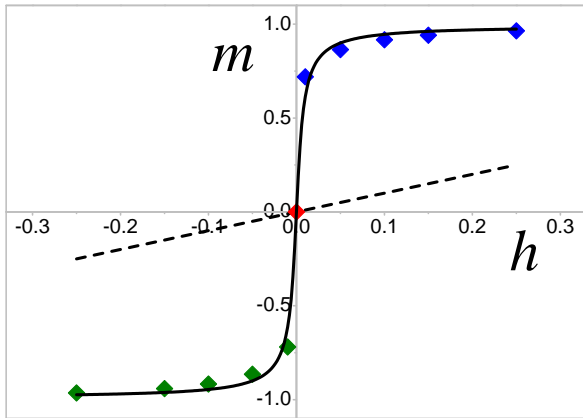


FIG. 4: The behavior of $\langle X \rangle$ for various systems with $N_I + N_E = 200$, displayed in terms of $m(h)$. Green (blue) diamonds are associated with N_I (N_E) being 125, 115, 110, 105, and 101. The red diamond is the symmetric, critical case of (100, 100). The dashed line is the prediction from an ‘intuitively reasonable’ argument. A mean-field approach leads to the solid (black) line.

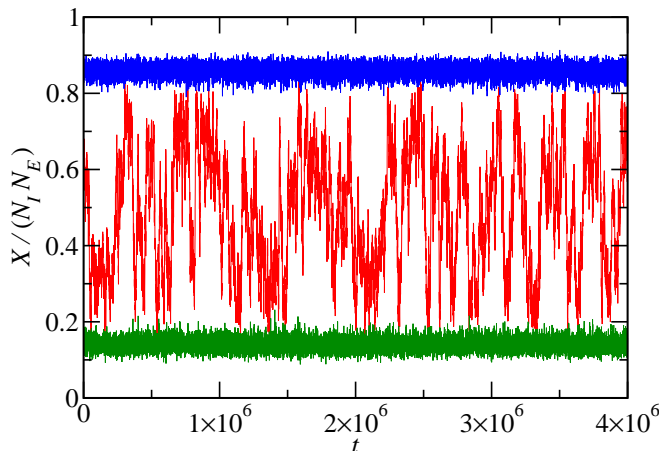


FIG. 5: Time traces of X for three cases with (N_I, N_E) near/at criticality, shown in green (101, 99), red (100, 100), and blue (99, 101). To clarify, these are traces in the steady state, with $t = 0$ here being $\sim 10^8$ MCS after the start of the runs.

case $N_I = N_E = 100$ provide the motivation to study a simpler quantity. In XIE , a natural quantity is the total number of cross-links, X . Since it is a single number, studying X should be considerably easier. Furthermore, through the mapping to the Ising model, we recognize $2X - \mathcal{N}$ is the total magnetization M . Since the properties of M , especially its singular behavior near the critical point, have been extensively investigated, we believe that, by exploring a similar quantity in our system, we can benefit from known results. Unlike the Ising model however, there is essentially only one control parameter in XIE : $N_E - N_I$. The other, $\mathcal{N} = N_E N_I$ or $N = N_E + N_I$, should be regarded as the system size, suitable for finite-size scaling analysis. Of course, since we have defined a ‘Hamiltonian’ (Eqn. (8)), it would be natural to introduce a ‘temperature’ and consider \mathcal{P} ’s

like $\exp[-\mathcal{H}/k_B T]$ and perhaps some symmetry breaking variable as well. Such interesting questions are beyond the scope of this paper and will be pursued elsewhere. Here, let us focus on X and its response to $N_E - N_I$. By defining ‘intensive’ variables

$$m \equiv 2\langle X \rangle / \mathcal{N} - 1 \quad (22)$$

$$h \equiv (N_E - N_I) / (N_E + N_I) \quad (23)$$

we can pose our question as: What is the ‘equation of state’ $m(h)$ for the XIE model?

A. An extraordinary phase transition: Results from simulations and mean-field theory

To answer the question posed above, we can use the $\langle k_I \rangle$ from the simulation data above to construct $\langle X \rangle$ for the introverts and extroverts. Plotting the results in terms of $m(h)$, shown as solid diamonds in Fig. 4, we see that it deviates far from the naive expectation discussed above, namely, $\langle k_I \rangle = N_E^2 / N$, corresponding to $m = h$ and shown as the dashed black line. More remarkably, our $m(h)$ displays a sizeable jump – 70% of the full range when just two individuals ‘change sides’ (i.e., $(101, 99) \rightarrow (99, 101)$). Though such jumps resemble the equation of state for an Ising model with $T \ll T_c$, many aspects of our system do not display the typical characteristics of a first order transition, e.g., hysteresis, finite fluctuations, etc. The rest of this Subsection is devoted to different ways we probe this extraordinary transition. As we will see, despite the appearance of a discontinuity in $m(h)$, it is reasonable to refer to the $h \sim 0$ region as ‘critical,’ as typical behavior here conforms to that in systems displaying mixed-order transitions. Though discovered some time ago, such behavior is far less widely known as ordinary first and second order phase transitions [37].

1. Time traces, histograms, and power spectra

Since we collect time traces in a standard simulation, we should exploit the information they contain. Illustrated in Fig. 5 is $X(t)$ for the critical system, as well as the two neighboring cases: $h = 0, \pm 0.01$. Clearly, the trace for $N_I = N_E = 100$ (red line) is dramatically different from the other two. For $N_I = N_E \pm 2$, X settles down very quickly, hovering around the average $\langle X \rangle$ with fluctuations of $O(100)$ (i.e., $O(\sqrt{N})$ here). By contrast, in the critical case, X wanders widely (i.e., $O(N)$ here) and evolves exceedingly slowly. These time traces can be used to compile histograms in X , from which we obtain the steady state distribution $P(X)$, shown in Fig. 6. Not surprisingly, they are sharply peaked and Gaussian like for the off-critical cases (green and blue lines), while the distribution in the $N_I = N_E$ case (red line) is essentially flat over most of the full range, $[0, \mathcal{N}]$. Both the time trace of the critical case and the flat plateau in $P(X)$ give the impression of an *unbiased* random walk

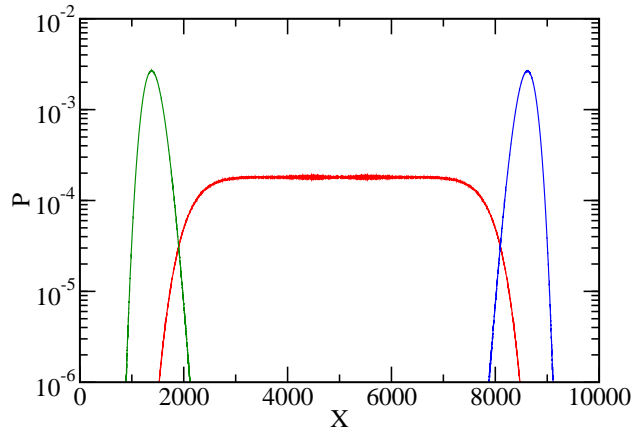


FIG. 6: The distribution, $P(X)$, compiled with the time traces in Fig. 5.

(RW), bounded by ‘soft’ walls near the extremes of the allowed region. By contrast, $M(t)$ for an Ising system below criticality spends much of its time hovering around the spontaneous magnetizations, $\pm M_{sp}$, and makes rare and short excursions from one to the other. Though not shown here, we observe no metastability when the two nodes ‘change sides’: $(101, 99) \rightarrow (99, 101)$. X/N simply marches from $\sim 15\%$ to $\sim 85\%$ in ~ 3500 MCS. In other words, on the average, X changes by about two links per MCS. We also considered having $\delta = 4$ or 6 ‘defectors’ instead of just two, in systems with $N = 400$ and 800 . In all cases, the average ‘velocity’ is approximately δ per MCS. Intuitively, we may attribute this to the action of the δ extra E nodes, but it remains to be shown analytically. In all respects, there is absolutely *no barrier* between the two extremes of X !

Finally, to confirm the notion of a RW, we compute the power spectrum of $X(t)$ as follows. With $\mathcal{T} = 2 \times 10^4$ measurements (of runs of 2×10^6 MCS), we compute the Fourier transform $X(\omega)$ and then average over 100 runs to obtain $I(\omega) \equiv \langle |X(\omega)|^2 \rangle$. In Fig. 7, we show plots of $\log I$ vs. $\log \omega$, as well a straight line (black dashed) representing ω^{-2} . The red data points, associated with $N_I = N_E = 100$, are statistically consistent with the RW characteristic of ω^{-2} . The cutoff at small ω can be estimated from the finite domain of the RW (~ 7000 here). Since $\Delta X = \pm 1$ in each attempt, we can assume the traverse time to be $\sim 7000^2 \cong 5 \times 10^7$ attempts, or $\sim 2.5 \times 10^5$ MCS. Given that this value is comparable to $1/10$ of our run time, it is reasonable to expect deviations from the pure ω^{-2} as we approach $\omega \sim 10$. By contrast, the power spectra of the two off-critical cases (green dots and blue line, from the green and blue traces in Fig. 5) are controlled by some intrinsic time scale associated with both the restoration to $\langle X \rangle$ and the fluctuations thereabout. Indeed, this $I(\omega)$ is entirely consistent with a Lorentzian, i.e., $\propto 1/(\omega^2 + \omega_0^2)$. Given our limited understanding of the dynamics of this model, estimating ω_0 is beyond the scope of this work. Let us remark that

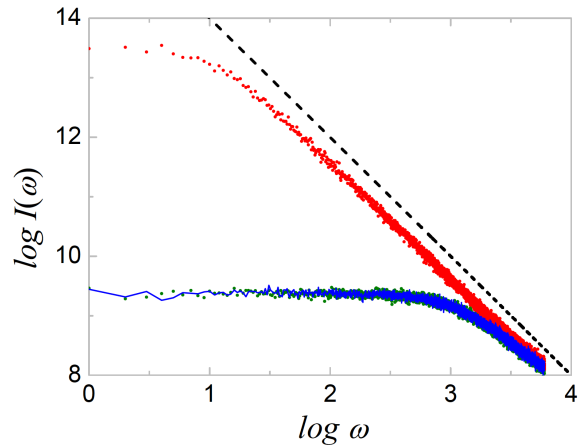


FIG. 7: Power spectra, $I(\omega)$, associated with the time traces in Fig. 5. The dashed black line is proportional to $1/\omega^2$. Note that the spectra associated with the two off-critical cases (shown as green dots and a blue line) are statistically identical, as expected from particle-hole symmetry.

we have preliminary data for systems of other sizes and that, while data collapse can be achieved, we have not found simple explanations for the parameters involved. Instead, we will present a brief phenomenological scaling analysis of one aspect of the critical system in Subsection 4.2. Here, let us turn to a mean-field approach which can provide some understanding of a number of these unusual properties.

2. Mean-field approximation

Unlike the complications we face with the degree distributions, it is simple to formulate a mean-field theory for X , directly from \mathcal{P}^{ss} . The underlying difference is that there is only one variable here and, in the spirit of the mean-field approximation, we can simply replace every n_{ij} by $\langle X \rangle / N$. Indeed, we may study the full (steady state) distribution of X , given exactly by

$$P(X) \equiv \sum_{\{\mathbf{N}\}} \delta(X, \Sigma_{ij} n_{ij}) \mathcal{P}^{ss}(\mathbf{N}). \quad (24)$$

Performing this sum to a closed form, however, is not feasible so far, since this task is comparable to finding $P(M)$ for the 2-dimensional Ising model. Therefore, we attempt a mean-field approach to make progress, replacing $k_i = \Sigma_j n_{ij}$ by $N_E (X/N) = X/N_I$ and $p_j = \Sigma_i n_{ij}$ by $N_I (1 - X/N) = N_I - X/N_E$. Meanwhile

$$\sum_{\{\mathbf{N}\}} \delta(X, \Sigma_{ij} n_{ij}) = \binom{N}{X} \quad (25)$$

so that our approximate distribution, \tilde{P} , is

$$\tilde{P}(X) \propto \binom{N}{X} \left(\left[\frac{X}{N_I} \right]! \right)^{N_I} \left(\left[N_I - \frac{X}{N_E} \right]! \right)^{N_E} \quad (26)$$

In this spirit, it is natural to consider

$$F(x; N_I, N_E) \equiv -\ln \tilde{P}(X) / \mathcal{N} \quad (27)$$

and regard it as a ‘Landau free energy density’ for the intensive variable

$$x \equiv X/\mathcal{N} \in [0, 1] \quad (28)$$

In the thermodynamic limit, the leading order of F is *linear* in x , with slope $\ln(N_I/N_E)$ [20, 25]. Thus, as long as $N_I \neq N_E$, x can only assume boundary values, 0 or 1, while, for $N_I = N_E$, F is *flat* over the entire interval. This prediction agrees qualitatively with the main simulation results, especially the evolution $\Delta X/\Delta t \sim \delta/\text{MCS}$ when $N_E = N_I - \delta$ is suddenly changed to $N_E = N_I + \delta$. Keeping the next order, $-\left(\frac{\ln x}{N_E} + \frac{\ln(1-x)}{N_I}\right)/2$, we find not only nonlinear terms, but also the necessary ‘repulsion’ to avoid the extremes. At this order, x settles within $O(1/N \ln[N_I/N_E])$ of the boundaries for generic $N_{I,E}$. Cast in the language of magnetism, $F(m; h, N)$ reads

$$\frac{m}{2} \ln \frac{1+h}{1-h} - \frac{1}{N} \left[\frac{\ln(1+m)}{1+h} + \frac{\ln(1-m)}{1-h} \right] + \dots$$

From here, we can find the minimum of F and obtain a mean-field ‘equation of state’:

$$m(h) \cong -H + \text{sign}(h) \sqrt{H^2 - 2Hh + 1} \quad (29)$$

where

$$H^{-1} = \frac{1}{2} N (1-h^2) \ln \frac{1+h}{1-h} = \frac{2N_E N_I}{N} \ln \frac{N_E}{N_I} \quad (30)$$

may be regarded as an alternate definition of a ‘magnetic field’ like control variable.

How does this prediction compare to data? For the specific case of $N = 200$, this $m(h)$ (solid black curve in Fig. 4) is remarkably close to the data points. Clearly, this mean-field approach captures some key features of the XIE model. We should caution the reader, however, that this plot shows a deceptively good agreement. Indeed, this prediction deviates from data (e.g., by as much as 3% for the (110, 90) case) considerably more than those from the self-consistent mean-field theory (where $\langle X \rangle = \langle k_I \rangle N_I$). Nor does the good agreement extend to the entire distribution: $\tilde{P}(X)$ deviates substantially from the histograms of X , especially for $N_E \cong N_I$. Nevertheless, it does offer some insight into the major differences between this system and an Ising ferromagnet at low temperatures. Note that, if the $N \rightarrow \infty$ limit is taken first in this approach, we find a highly singular $m(h) = \text{sign}(h)$. Work is in progress to explore the how such an extreme equation of state can be understood quantitatively in the context of an extreme Thouless effect [24].

B. A scaling study of the ‘critical’ system: $N_I = N_E$

In this subsection, we report preliminary results for a scaling study of the ‘critical’ system, $N_I = N_E$. For convenience, let us define $L \equiv N_{I,E} = N/2$, so that we can

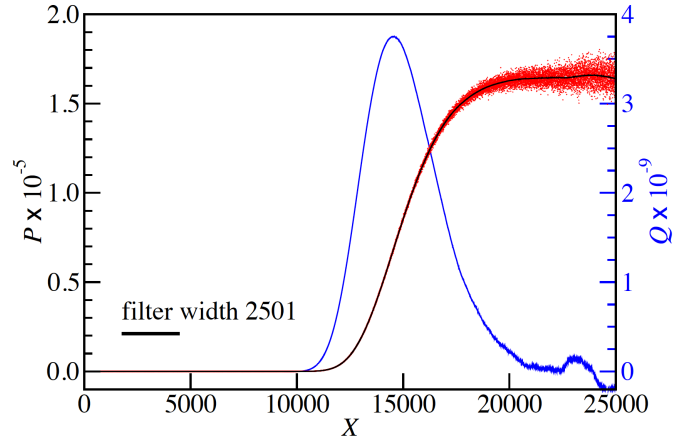


FIG. 8: Determining the location of the edge of the plateau of the distribution $P(X)$. An example of the use of Savitzky-Golay filtering to find $P(X)$ (black dashed line) and its derivative $Q(X)$ (blue solid line) from data for system size $N = 316$ shown as the (red) scattered points. A filter width slightly less than the full width at half maximum of the peak of $Q(X)$ was used.

regard our system as an $L \times L$ Ising model with $\mathcal{N} = L^2$ ‘spins’ while $M = 2X - L^2$ is its total magnetization. As can be seen in Fig. 6, the distribution $P(X)$ displays a broad plateau. In terms of the fraction X/\mathcal{N} , the width of the plateau increases with L . We perform extensive simulations to investigate this phenomenon quantitatively. Specifically, we determine the location of the left edge of the plateau as a function of L , defined as the value of X ($< \mathcal{N}/2$) where P has vanishing curvature. Thus, let us define $X_{Q_{\max}}(L)$ as the value where

$$Q(X) = \frac{dP(X)}{dX}$$

reaches a maximum value. Determining $X_{Q_{\max}}$ from simulations accurately poses two challenges, especially for large L . First, in the critical state, X performs a RW over the plateau, spending little time near the edges. Thus obtaining good statistics for $P(X)$ near the edges is difficult. Second, taking numerical derivatives of noisy data to obtain an accurate estimate of $Q(X)$ is non-trivial. We have utilized specialized numerical methods in an effort to address both of these difficulties.

In order to alleviate the first difficulty, we exploited the fact that the original dynamics sends our system to an equivalent equilibrium system with a Hamiltonian given by Eqn. (8) (and unit temperature in the Boltzmann factor). Thus, we are allowed to bias the dynamics by adding an additional term

$$\Delta \mathcal{H}(X) = \mu |X - \mathcal{N}/2|$$

to \mathcal{H} . With $\mu > 0$, this extra term biases the system towards the edges of the plateau in $P(X)$, against spending time in the center. As a result, in a simulation of the modified system, the region near the edges is sampled much more frequently, providing much better statistics. To recover the desired $P(X)$, from $P_{\Delta \mathcal{H}}(X)$, the distribution of the modified system requires a simple reweighting

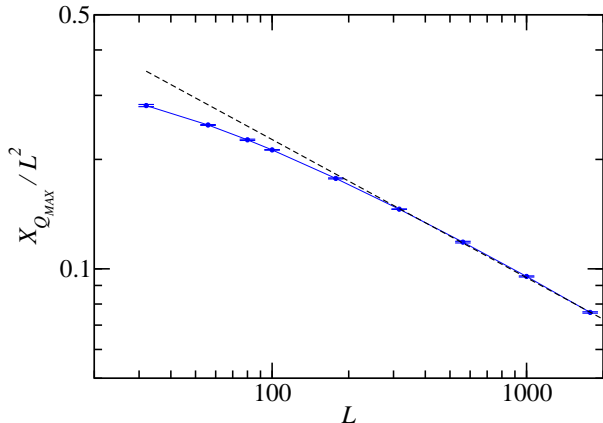


FIG. 9: Scaling behavior of $X_{Q_{\max}}$: the location of the edge of the plateau of the distribution $P(X)$ as a function of system size N .

[30]:

$$P(X) \propto P_{\Delta\mathcal{H}}(X) e^{-\Delta\mathcal{H}(X)}.$$

Even with such improvements, the data for $P(X)$ is still quite noisy for the purpose of obtaining its derivative Q reliably. One possibility is to simply bin the data for $P(X)$, but this procedure could shift the location of $X_{Q_{\max}}$. To overcome this second difficulty, we smooth the data using *Savitzky-Golay filtering* (SGf) [31, 32]. This method of filtering performs a least-squares fit of a polynomial function over a moving window, the ‘filter width’, of the data. A particularly useful feature of SGf, as opposed to other related filtering methods, is that it efficiently produces a smoothed derivative function that fits the data as well as the function itself. An example of our use of SGf is shown in Fig. 8. In the figure, we show the reweighted data for $P(X)$ (for $L = 316$), as well as the results for the fitted functions $P(X)$ and $Q(X)$. We explore using polynomials of different order and using different filter widths in our smoothing process. For the sigmoidal shaped data we have, we find stable results for locating $X_{Q_{\max}}$ by using a fourth-order polynomial and a filter width that is slightly less than the full width at half maximum of the peak in $Q(X)$.

Using these methods, we determine $X_{Q_{\max}}(L)$ for L ranging from 32 to 1778. For each system size, we carry out three to five different simulation runs, ranging from 10^{11} MCS for the small systems to 5×10^9 MCS for the largest. The values of μ used in the modified simulations and subsequent reweighting vary from about 10^{-3} for $L = 100$ (modified simulations are not used on smaller systems) to about 10^{-6} for $L = 1778$. Each run is analyzed separately, so that we have an estimate of the statistical errors. The results are shown as a log-log plot of $X_{Q_{\max}}/L^2$ vs. L in Fig. 9. The error bars indicate the 2σ statistical errors in the variation of the results from the different runs. Systematic errors associated with changing the filtering parameters are in the same range. The straight line in the figure has a slope of -0.38 . The con-

clusion is that, for large systems, the *fraction* of cross-links at the left edge of $P(X)$ scales as a power of L :

$$\frac{X_{Q_{\max}}}{L^2} \sim L^{-0.38}.$$

Of course, it is difficult to compare such a result to those from the mean-field theory above. Clearly, despite its minimal nature, this system displays a variety of rich behavior, understanding which will require, at the least, a detailed finite size analysis.

V. SUMMARY AND OUTLOOK

In this article, we continue our study of preferred degree networks and the interaction between such networks, but focus on a particular limit, with *extreme* introverts and extroverts (i.e., $\kappa_I = 0$ and $\kappa_E = \infty$, respectively). In this minimal model, there are only two control parameters, $N_{I,E}$, the number of I ’s and E ’s. Since they only cut or add connections if possible, the intra-community links quickly empty/fill and become frozen. As only the cross-links are active, each configuration of the network can be completely specified by an incidence matrix, \mathbb{N} . ($n_{ij} = 1, 0$ for the presence or absence of a link between nodes i and j). Though the dynamics of interacting networks of this class does not generally obey detailed balance, it is restored in this limit, so that we are able to find an analytic expression for the stationary, microscopic distribution, $\mathcal{P}(\mathbb{N})$. Since the elements of \mathbb{N} are binary, our system can be regarded as a kinetic Ising model and $-\ln \mathcal{P}$ can be thought of as a ‘Hamiltonian’ \mathcal{H} . In this language, our system displays peculiar long range, ‘multi-spin’ interactions, unlike any magnetic systems in nature. Like the Ising model, a particle-hole symmetry prevails here, though it is slightly more obscure.

Our simulation study of its collective behavior focuses on the degree distributions and X , the total number of cross-links, relying mostly on systems with $N_I + N_E = 200$. The most remarkable aspect is that, even when $N_I \cong N_E$, the fraction of cross-links is far from the symmetric value of $1/2$. Instead, there is a sizeable jump as N_I crosses N_E , e.g., from $\sim 15\%$ to $\sim 85\%$ when just two nodes ‘change sides’ ($(101, 99) \rightarrow (99, 101)$). The nature of this transition fails to conform to the standard categories of first or second order. On one hand, the sizeable jump of $\langle X \rangle$ suggests a first order phase transition. Yet, the other features typically associated with first order phase transitions are absent here, such as metastability, hysteresis, phase co-existence, etc. On the other hand, the extensive fluctuations and slow dynamics are more typical of a system at a second order transition. Most likely, it belongs to the class of less well-known, mixed-order transitions. Indeed, it is very likely that the XIE displays an ‘extreme’ Thouless effect [24], in that the jump of $\langle X \rangle / \mathcal{N}$ will cover the entire unit interval as $N \rightarrow \infty$. We expect such behavior from the limited finite size analysis presented here, namely, the left edge of the plateaux in $P(X)$ for the symmetric case

decreases as $1/N^{0.38}$. Work towards a more systematic study of finite size scaling is in progress [33]. Naturally, these extraordinary aspects are expected to manifest in the more detailed degree distributions. So far, apart from the $N_I = N_E$ case, the degree distributions can be reasonably well predicted by a self-consistent mean-field approach. A less refined, but more accessible, approximation scheme is presented for describing the behavior of X . Though less accurate, this scheme offers some insight into the puzzling features associated with the transition. There is clearly room for quantitative improvements. Naturally, these extraordinary aspects are also manifest in the more detailed degree distributions. Apart from the $N_I = N_E$ case, the degree distributions can be reasonably well predicted by a self-consistent mean field approach. A less refined, but more accessible, approximation scheme is presented for describing the behavior of X . Though less accurate, this scheme offers some insight into the puzzling features associated with the transition.

This remarkably simple, yet quite rich, system deserves to be investigated further. The most obvious question may be whether a thermodynamic limit exists, and in what way. For example, do the degree distributions approach a non-trivial limit when $N \rightarrow \infty$? with N_I/N_E held fixed or with $N_I - N_E$ being a constant? as a function of k, p or some scaled variable? Despite the presence of an explicit expression for the microscopic distribution and its associated \mathcal{H} , computing the partition function, let alone averages of quantities of interest, poses a worthy challenge. The failure of mean-field theory, especially near ‘criticality’ hints at the importance of correlations. Preliminary studies indicate strong correlations, in the sense that the difference between the joint distribution, $\rho(k_I, k_E)$, and the product $\rho_I(k_I)\rho_E(k_E)$ can be a sizeable fraction of the former. Systematic investigations of them are straightforward and surely worthwhile. Presumably, once some progress along these directions is made, it is possible to investigate the more serious issues concerning the nature of the mixed-order transition. For example, can we understand and predict the absence of *any* barrier (in the symmetric system) between the degenerate extremes? Launching a systematic study of finite size scaling will also help to shed light on such peculiarities of this model. Of course, we should also pursue the questions raised above, e.g., details of the power spectra, especially for systems with $N_I \neq N_E$. In an earlier paper of this series [23], we introduced a quantitative concept of ‘frustration’ (in the ordinary psychological sense). Though *XIE* seems to be a maximally frustrated model, its role and behavior are yet to be considered.

Beyond exploring these questions, we can extend the *XIE* mode in an orthogonal direction, arguably of purely theoretical interest (at present). We may treat \mathcal{H} as a genuine Hamiltonian in a standard study of critical phenomena in thermal equilibrium. In other words, we propose to study the statistical mechanics of a $L \times L$ system associated with the Boltzmann factor

$$\mathcal{P} \propto \exp \{-\beta [\mathcal{H} - BX]\} \quad (31)$$

where B plays the role of a symmetry breaking, ‘magnetic

field’ (as opposed to h in the *XIE*). It is interesting to note that, while the critical control parameters of a typical system (e.g., T_c in Ising, T_c and P_c for liquid gas) are not known, they are given precisely by $\beta_c = 1$ and $B_c = 0$ here. For this ‘purely theoretical’ system, work is in progress [33] to explore the usual avenues of interest: static and dynamic critical exponents, scaling functions, universality and the classes, etc. In the context of renormalization group analyses (which proved to be highly effective in dealing with other mixed-order transitions [24]), we already know that \mathcal{H} lies on the critical sheet and can inquire about fixed points and their neighborhoods, irrelevant and relevant variables (e.g., if there are others besides $\beta - 1$ and B). Similarly, we might ask if the perspectives from catastrophe theory [34] can offer fresh insight.

Beyond the *XIE* and its companion model, there is a wide vista involving dynamic networks with preferred degrees. For instance, instead of assigning one or two κ ’s to a population, it is surely more natural to assign a distribution of κ ’s. There are also multiple ways to model interactions between the various groups. For example, even with just two groups, it is realistic to believe that an individual may have *two* preferred degrees, one for contacts within the group and another for those outside. Surely, this kind of differential preference underlies the formation of social cliques. Beyond understanding the topology and dynamics of interacting networks of the types described here, the next natural step is to take into account the freedom associated with the nodes, e.g., opinion, wealth, health, etc., on the way to the ambitious goal of understanding adaptive, co-evolving, interdependent networks in general.

Appendix A: Restoration of detailed balance

In this appendix, we show that all Kolmogorov loops are reversible in the *XIE* model and so, detailed balance is restored [35]. Since the full dynamics occurs on the \mathcal{N} cross-links, the configuration space consists of the corners of an \mathcal{N} -dimensional unit cube, while adding/cutting a link is associated to traverse along an edge therein. Clearly, products of the ratios of forward and reversed transition rates around any closed loop can be expressed in terms of those around ‘elementary loops’ – i.e., loops around a plaquette on the \mathcal{N} -cube. We will show that the ratio associated with every plaquette is unity and so, all Kolmogorov loops are reversible.

First, it is easy to see that if an elementary loop consists of modifying two links connected to four different nodes, then the actions on each link are unaffected by the other. In other words, rates associated with opposite sides of the square (loop) are the same. Thus, their product in one direction is necessarily the same as in the reverse. We need to focus only on situations where the two links are connected to three nodes, e.g., ij and im . For any such loop, let us start with a configuration in which both are absent ($n_{ij} = n_{im} = 0$). Let the states

of node be such that i has k_i links, and j and m have p_j and p_m ‘holes’, respectively. Then one way around the loop is adding these two links followed by cutting them, which can be denoted as the sequence

$$\begin{pmatrix} n_{ij} \\ n_{im} \end{pmatrix} = \begin{pmatrix} 0 \\ 0 \end{pmatrix} \rightarrow \begin{pmatrix} 1 \\ 0 \end{pmatrix} \rightarrow \begin{pmatrix} 1 \\ 1 \end{pmatrix} \rightarrow \begin{pmatrix} 0 \\ 1 \end{pmatrix} \rightarrow \begin{pmatrix} 0 \\ 0 \end{pmatrix} \quad (\text{A1})$$

and leaving the rest of \mathbb{N} unchanged. The associated product of the transition rates is, apart from an overall factor of N^4 ,

$$\frac{1}{p_j} \frac{1}{p_m} \frac{1}{k_i + 2} \frac{1}{k_i + 1} \quad (\text{A2})$$

Now, the reversed loop can be denoted as

$$\begin{pmatrix} n_{ij} \\ n_{im} \end{pmatrix} = \begin{pmatrix} 0 \\ 0 \end{pmatrix} \rightarrow \begin{pmatrix} 0 \\ 1 \end{pmatrix} \rightarrow \begin{pmatrix} 1 \\ 1 \end{pmatrix} \rightarrow \begin{pmatrix} 1 \\ 0 \end{pmatrix} \rightarrow \begin{pmatrix} 0 \\ 0 \end{pmatrix} \quad (\text{A3})$$

associated with the product

$$\frac{1}{p_m} \frac{1}{p_j} \frac{1}{k_i + 2} \frac{1}{k_i + 1} \quad (\text{A4})$$

which is exactly equal to Eqn. (A2). From symmetry, we can expect the same results for loops involving two introverts and one extrovert (i.e., ij and kj). Thus, we conclude that the Kolmogorov criterion is satisfied and detailed balance is restored in this XIE limit. Our system should settle into a stationary distribution without probability currents, much like the Boltzmann distribution for a system in thermal equilibrium.

Acknowledgments

We thank D. Dhar, Y. Kafri, W. Kob, D. Mukamel, Z. Toroczkai for illuminating discussions. This research is supported in part by the US National Science Foundation, through grants DMR-1206839 and DMR-1244666, and (KEB) by AFOSR and DARPA through grant FA9550-12-1-0405. One of us (RKPZ) thanks the Galileo Galilei Institute for Theoretical Physics for hospitality and the INFI for partial support during the completion of this paper.

-
- [1] Strogatz S H 2001 *Nature* **410** 268
 - [2] Albert R and Barabási A-L 2002 *Rev. Mod. Phys.* **74** 47
 - [3] Dorogovtsev S N, Mendes J F F 2002 *Adv. Phys.* **51** 1079
 - [4] Newman M E J 2003 *SIAM Rev.* **45** 167
 - [5] Estrada E, Fox M, Higham D and Oppo G-L (eds) 2010 *Network Science: Complexity in Nature and Technology* (Springer, New York)
 - [6] Barrat A, Barthélemy M, Vespignani A 2008 *Dynamical processes on complex networks* (Cambridge University Press)
 - [7] Dorogovtsev S N, Goltsev A V and Mendes J F F 2008 *Rev. Mod. Phys.* **80** 1275
 - [8] Gross T, D’Lima C J D and Blasius B 2006 *Phys. Rev. Lett.* **96** 208701
 - [9] Gross T and Blasius B 2008 *J. R. Soc. Interface* **5** 259
 - [10] Rinaldi S, Peerenboom J and Kelly T 2001 *IEEE Contr. Syst. Mag.* **21** 11
 - [11] Panziera S, Setola R 2008 *Int. J. Model. Ident. Contr.* **3** 69
 - [12] Buldyrev S V, Parshani R, Paul G, Stanley H E and Havlin S 2010 *Nature (London)* **464** 1025
 - [13] Vespignani A 2010 *Nature (London)* **464** 984
 - [14] Buldyrev S V, Shere N W and Cwiliich G A 2011 *Phys. Rev. E* **83** 016112
 - [15] Kurant M and Thiran P 2006 *Phys. Rev. Lett.* **96** 138701
 - [16] Liu M and Bassler K E 2006 *Phys. Rev. E* **74** 041910
 - [17] Del Genio C I and Gross T 2011 *New J. Phys.* **13** 103038
 - [18] Platini T and Zia R K P 2010 *J. Stat. Mech. Theory Exp.* **2010** P10018
 - [19] Zia R K P, Liu W, Jolad S, and Schmittmann B 2011 *Physics Procedia* **15** 102
 - [20] Zia R K P, Liu W, and Schmittmann B 2012 *Physics Procedia* **34** 124
 - [21] Jolad S, Liu W, Schmittmann B and Zia R K P 2012 *PLoS ONE* **7(11)** e48686
 - [22] Liu W, Jolad S, Schmittmann B and Zia R K P 2013 *J. Stat. Mech. Theory Exp.* **2013** P08001
 - [23] Liu W, Schmittmann B and Zia R K P 2014 *J. Stat. Mech. Theory Exp.* **2014** P05021
 - [24] Bar A and Mukamel D 2014 *Phys. Rev. Lett.* **112** 015701
 - [25] Liu W, Schmittmann B and Zia R K P 2012 *EPL* **100** 66007
 - [26] Erdős P and Rényi A 1959 *Pub. Math.* **6** 290
 - [27] Zia R K P and Schmittmann B 2007 *J. Stat. Mech. Theory Exp.* **2007** P07012
 - [28] Glauber R J 1963 *J. Math. Phys.* **4** 294
 - [29] Yang C N and Lee T D 1952 *Phys. Rev.* **87** 410
 - [30] Ferrenberg A M and Swendsen R H 1988 *Phys. Rev. Lett.* **61** 2635
 - [31] Savitzky A and Golay M J E 1964 *Anal. Chem.* **8** 1627
 - [32] Press W H, Teukolsky S A, Vetterling W T and Flannery B P 2007 *Numerical Recipes - The Art of Scientific Computing* (3rd ed.) (Cambridge University Press) 771
 - [33] Bassler K E and Zia R K P 2014 unpublished
 - [34] Thom R 1975 *Structural Stability and Morphogenesis: An Outline of a General Theory of Models* (W. A. Benjamin, Reading, MA)
 - [35] Kolmogorov A N 1936 *Math. Ann.* **112** 155
 - [36] Of course, $\ln(\sum_j n_{ij})!$ can be cast as $\sum_\ell \ln(\sum_j n_{ij} - \ell)$ but this form is hardly a simplification.
 - [37] An excellent summary of the Thouless effect can be found in ref.[24].